

Influence of the nuclear equation of state on the hadron-quark phase transition in neutron stars^{*}

YANG Fang(杨芳)¹⁾ SHEN Hong(申虹)²⁾

(Department of Physics, Nankai University, Tianjin 300071, China)

Abstract We study the hadron-quark phase transition in the interior of neutron stars, and examine the influence of the nuclear equation of state on the phase transition and neutron star properties. The relativistic mean field theory with several parameter sets is used to construct the nuclear equation of state, while the Nambu-Jona-Lasinio model is used for the description of the deconfined quark phase. Our results show that a harder nuclear equation of state leads to an earlier onset of a mixed phase of hadronic and quark matter. We find that a massive neutron star possesses a mixed phase core, but it is not dense enough to possess a pure quark core.

Key words hadron-quark phase transition, equation of state, neutron stars

PACS 26.60.+c, 24.10.Jv, 24.85.+p

1 Introduction

The study of the hadron-quark phase transition at high density is of great interest in both nuclear physics and astrophysics. It is expected that the deconfinement phase transition occurs in the core of massive neutron stars^[1]. It has been pointed out by Glendenning^[2] that the hadron-quark phase transition in neutron stars may proceed through a mixed phase of hadronic and quark matter over a finite range of pressures and densities according to the Gibbs criteria for phase equilibrium. Such phase transition has received much attention in neutron star physics^[3–7]. In general, the presence of the quark degree of freedom tends to soften the equation of state (EOS) at high density and lower the maximum mass of neutron stars.

In order to investigate the hadron-quark phase transition, we need models to describe hadronic matter and quark matter. Unfortunately, there is no single model which can be used to describe both phases and the dynamic process of the phase transition. We have to use different approaches for the description of the two phases, and then perform the Glendenning construction for the charge-neutral mixed phase

where both hadronic and quark phases coexist^[2]. In this work, we adopt the relativistic mean field (RMF) theory to describe the hadronic matter phase, while the Nambu-Jona-Lasinio (NJL) model is used for the quark matter phase. The RMF theory has been quite successfully and widely used for the description of nuclear matter and finite nuclei^[8–12]. It has also been applied to provide the equation of state of dense matter for the use in supernovae and neutron stars^[13, 14]. There are many parameter sets of the RMF model in the literature, which are fitted to some nuclear matter properties or ground-state properties of finite nuclei. In order to evaluate the sensitivity of the results to the parameters used in the RMF model, we employ four different parameter sets, namely, NL3^[15], TM1^[16], GM1^[17], and GPS^[18]. For the quark phase we adopt a two-flavor version of the NJL model^[19]. The choice of the NJL model is motivated by the fact that this model can successfully reproduce many aspects of quantum chromodynamics such as the non-perturbative vacuum structure and dynamical breaking of chiral symmetry^[19–21]. With a definite EOS for quark matter based on the NJL model, we examine the influence of the hadronic EOS on the hadron-quark phase transition and neutron star properties.

Received 11 September 2007

^{*} Supported by National Natural Science Foundation of China (10675064) and Specialized Research Fund for the Doctoral Program of Higher Education (20040055010)

1) E-mail: yangfang022@mail.nankai.edu.cn

2) E-mail: songtc@nankai.edu.cn

For a comprehensive description of neutron stars, we need not only the EOS at high density for the interior region but also the EOS for the inner and outer crusts, where the density is low and heavy nuclei exist. For the nonuniform matter at low density, we adopt a relativistic EOS based on the RMF theory with a local density approximation^[13, 14]. The nonuniform matter is modelled to be composed of a lattice of spherical nuclei immersed in an electron gas with or without free neutrons dripping out of nuclei. As the density increases, heavy nuclei dissolve and the optimal state is a uniform matter consisting of neutrons, protons, and leptons (electrons and muons) in β equilibrium. The low density EOS is therefore matched to an EOS of uniform nuclear matter at around 10^{14} g/cm³^[14]. As for the EOS at high density, there are many discussions in the literature about possible mechanisms to soften the EOS, e.g., by hyperons, kaon condensation, and/or quark matter^[4–7, 19, 22]. In this paper, we would like to focus on the study of the hadron-quark phase transition, so the hadronic matter in the present calculation is restricted to nucleonic degrees of freedom only. Applying the EOS of neutron star matter over a wide density range, we study the neutron star properties by solving the Tolman-Oppenheimer-Volkoff equation, and examine whether or not quark matter can exist in the core of neutron stars.

This paper is arranged as follows. In Sec. 2, we discuss the EOS for hadronic matter in the RMF theory. In Sec. 3, the NJL model is used for the description of quark matter. In Sec. 4, we investigate the hadron-quark phase transition of neutron star matter, and examine the influence of the hadronic EOS. We present in Sec. 5 the properties of neutron stars. Sec. 6 is devoted to a summary.

2 Hadronic phase

We adopt the relativistic mean field (RMF) theory to describe the hadronic matter phase. In the RMF theory, baryons interact via the exchange of isoscalar scalar and vector mesons (σ and ω) and isovector vector meson ρ , which are treated as classical fields in the mean-field approximation. For neutron star matter consisting of a neutral mixture of nucleons (p and n) and leptons (e and μ) in β equilibrium, we start from the effective Lagrangian

$$\begin{aligned} \mathcal{L}_{\text{RMF}} = & \sum_{b=n,p} \bar{\psi}_b [i\gamma_\mu \partial^\mu - m_N - g_\sigma \sigma - g_\omega \gamma_\mu \omega^\mu - \\ & g_\rho \gamma_\mu \tau_a \rho^{a\mu}] \psi_b + \frac{1}{2} \partial_\mu \sigma \partial^\mu \sigma - \frac{1}{2} m_\sigma^2 \sigma^2 - \\ & \frac{1}{3} g_2 \sigma^3 - \frac{1}{4} g_3 \sigma^4 - \frac{1}{4} W_{\mu\nu} W^{\mu\nu} + \frac{1}{2} m_\omega^2 \omega_\mu \omega^\mu + \end{aligned}$$

$$\begin{aligned} & \frac{1}{4} c_3 (\omega_\mu \omega^\mu)^2 - \frac{1}{4} R_{\mu\nu}^a R^{a\mu\nu} + \frac{1}{2} m_\rho^2 \rho_\mu^a \rho^{a\mu} + \\ & \sum_{l=e,\mu} \bar{\psi}_l [i\gamma_\mu \partial^\mu - m_l] \psi_l, \end{aligned} \quad (1)$$

where the notation follows the standard one^[13]. The parameters in the Lagrangian are usually determined by fitting to nuclear matter properties or ground-state properties of finite nuclei. There are several parameter sets which are often used in the RMF calculations. Here we employ four different parameter sets, NL3^[15], TM1^[16], GM1^[17], and GPS^[18], as listed in Table 1, so as to evaluate the sensitivity of the results to the RMF parameter set used. The nuclear matter properties of these parameter sets are shown in Table 2.

Table 1. The parameter sets of the RMF model used in the calculation. The masses are given in MeV.

set	NL3	TM1	GM1	GPS
Ref.	[15]	[16]	[17]	[18]
m_N	939.0	938.0	938.0	938.0
m_σ	508.194	511.198	550.0	550.0
m_ω	782.501	783.0	783.0	783.0
m_ρ	763.0	770.0	770.0	770.0
g_σ	10.217	10.0289	9.5705	8.1223
g_ω	12.868	12.6139	10.6096	8.2817
g_ρ	4.474	4.6322	4.0977	4.3736
g_2/fm^{-1}	-10.431	-7.2325	-12.2799	-5.3083
g_3	-28.885	0.6183	-8.9767	120.9956
c_3	-	71.3075	-	-

Table 2. The nuclear matter properties of the parameter sets used in the calculation. The saturation density and the energy per particle are denoted by n_0 and E/A , the incompressibility by K , the effective mass by m_N^* , and the symmetry energy by a_{sym} .

set	NL3	TM1	GM1	GPS
n_0/fm^{-3}	0.148	0.145	0.153	0.150
$(E/A)/\text{MeV}$	-16.3	-16.3	-16.3	-16.0
K/MeV	272	281	300	300
m_N^*/m_N	0.60	0.63	0.70	0.80
$a_{\text{sym}}/\text{MeV}$	37.4	36.9	32.5	32.5

Considering a homogeneous matter, the meson field equations at the mean-field level have the following form:

$$m_\sigma^2 \sigma + g_2 \sigma^2 + g_3 \sigma^3 = - \sum_{b=n,p} \frac{g_\sigma}{\pi^2} \int_0^{k_F^b} \frac{m_N^* k^2}{\sqrt{k^2 + m_N^{*2}}} dk, \quad (2)$$

$$m_\omega^2 \omega + c_3 \omega^3 = \sum_{b=n,p} \frac{g_\omega (k_F^b)^3}{3\pi^2}, \quad (3)$$

$$m_\rho^2 \rho = \sum_{b=n,p} \frac{g_\rho \tau_3^b (k_F^b)^3}{3\pi^2}, \quad (4)$$

where $\sigma = \langle \sigma \rangle$, $\omega = \langle \omega^0 \rangle$, and $\rho = \langle \rho^{30} \rangle$ are the expectation values of the meson fields. $m_N^* = m_N + g_\sigma \sigma$ is the effective nucleon mass, and k_F^b is the Fermi momentum of protons ($b = p$) or neutrons ($b = n$). τ_3^b

denotes the isospin projection of protons or neutrons. For neutron star matter containing nucleons and leptons, the conditions of β equilibrium and charge neutrality should be satisfied. The β equilibrium conditions without trapped neutrinos are given by

$$\mu_p = \mu_n - \mu_e, \quad (5)$$

$$\mu_\mu = \mu_e, \quad (6)$$

where μ_i is the chemical potential of species i . At zero temperature, the chemical potentials of nucleons and leptons are expressed by

$$\mu_b = \sqrt{k_F^b{}^2 + m_N^{*2}} + g_\omega \omega + g_\rho \tau_3^b \rho, \quad (7)$$

$$\mu_l = \sqrt{k_F^l{}^2 + m_l^2}. \quad (8)$$

The charge neutrality condition is given by

$$n_p = n_e + n_\mu, \quad (9)$$

where $n_i = (k_F^i)^3 / (3\pi^2)$ is the number density of species i . The coupled Eqs. (2)–(6) and (9) can be solved self-consistently at a given baryon density $n_B = n_p + n_n$. The total energy density and pressure of neutron star matter are given by

$$\begin{aligned} \varepsilon_{\text{HP}} = & \sum_{b=n,p} \frac{1}{\pi^2} \int_0^{k_F^b} \sqrt{k^2 + m_N^{*2}} k^2 dk + \\ & \frac{1}{2} m_\sigma^2 \sigma^2 + \frac{1}{3} g_2 \sigma^3 + \frac{1}{4} g_3 \sigma^4 + \\ & \frac{1}{2} m_\omega^2 \omega^2 + \frac{3}{4} c_3 \omega^4 + \frac{1}{2} m_\rho^2 \rho^2 + \\ & \sum_{l=e,\mu} \frac{1}{\pi^2} \int_0^{k_F^l} \sqrt{k^2 + m_l^2} k^2 dk, \quad (10) \end{aligned}$$

$$\begin{aligned} P_{\text{HP}} = & \frac{1}{3} \sum_{b=n,p} \frac{1}{\pi^2} \int_0^{k_F^b} \frac{k^4 dk}{\sqrt{k^2 + m_N^{*2}}} - \\ & \frac{1}{2} m_\sigma^2 \sigma^2 - \frac{1}{3} g_2 \sigma^3 - \frac{1}{4} g_3 \sigma^4 + \\ & \frac{1}{2} m_\omega^2 \omega^2 + \frac{1}{4} c_3 \omega^4 + \frac{1}{2} m_\rho^2 \rho^2 + \\ & \frac{1}{3} \sum_{l=e,\mu} \frac{1}{\pi^2} \int_0^{k_F^l} \frac{k^4 dk}{\sqrt{k^2 + m_l^2}}. \quad (11) \end{aligned}$$

3 Quark phase

In this section, we use a two-flavor version of the NJL model to describe the deconfined quark phase. The Lagrangian is given by

$$\mathcal{L}_{\text{NJL}} = \bar{q} (i\gamma_\mu \partial^\mu - m^0) q + G [(\bar{q}q)^2 + (\bar{q}^i \gamma_5 \tau q)^2], \quad (12)$$

where q denotes a quark field with two flavors ($N_f = 2$) and three colors ($N_c = 3$). G is a dimensionful cou-

pling constant (mass⁻²) and τ is a Pauli matrix acting in flavor space. $m^0 = \text{diag}(m_u^0, m_d^0)$ contains the current quark masses, and we assume the isospin symmetry $m_u^0 = m_d^0 \equiv m_q^0$. The model has three parameters: the current quark mass m_q^0 , the coupling constant G , and the momentum cutoff Λ . In the present calculation, we adopt the parameter set given in Ref. [19], $m_q^0 = 5.6$ MeV, $\Lambda = 587.9$ MeV, and $G\Lambda^2 = 2.44$, which are chosen to reproduce empirical values for the pion mass and decay constant in vacuum.

In the NJL model, the quarks get constituent quark masses by spontaneous chiral symmetry breaking. The constituent quark mass in vacuum m_q is much larger than the current quark mass m_q^0 . In the quark matter at high density, the constituent quark mass m_q^* becomes approximately the same as m_q^0 , which reflects the restoration of chiral symmetry. Within the mean-field approximation, m_q^* is obtained by solving the gap equation

$$m_q^* = m_q^0 - 2G(C_u + C_d), \quad (13)$$

where the quark condensate $C_i = \langle \bar{q}_i q_i \rangle$ is given by

$$C_i = -\frac{3}{\pi^2} \int_{k_F^i}^{\Lambda} \frac{m_q^*}{\sqrt{k^2 + m_q^{*2}}} k^2 dk. \quad (14)$$

Here, k_F^i denotes the Fermi momentum of the quark flavor i ($i = u$ or d), which is connected with the number density n_i and the chemical potential μ_i via

$$n_i = \frac{(k_F^i)^3}{\pi^2}, \quad (15)$$

$$\mu_i = \sqrt{k_F^i{}^2 + m_q^{*2}}. \quad (16)$$

The energy density of the quark system is given by

$$\begin{aligned} \varepsilon_{\text{NJL}} = & \sum_{i=u,d} \left[-\frac{3}{\pi^2} \int_{k_F^i}^{\Lambda} \sqrt{k^2 + m_q^{*2}} k^2 dk \right] + \\ & G(C_u + C_d)^2 - \varepsilon_0, \quad (17) \end{aligned}$$

where ε_0 is introduced to ensure $\varepsilon_{\text{NJL}} = 0$ in the vacuum.

For the quark matter consisting of a neutral mixture of quarks (u and d) and leptons (e and μ) in β equilibrium, the charge neutrality condition is expressed as

$$\frac{2}{3} n_u - \frac{1}{3} n_d - n_e - n_\mu = 0, \quad (18)$$

the β equilibrium conditions are given by

$$\mu_d = \mu_u + \mu_e, \quad (19)$$

$$\mu_\mu = \mu_e. \quad (20)$$

We solve the coupled Eqs. (13) and (18)–(20) at a given baryon density $n_B = (n_u + n_d)/3$. The total energy density and pressure including the contributions

from both quarks and leptons are given by

$$\varepsilon_{\text{QP}} = \varepsilon_{\text{NJL}} + \sum_{l=e,\mu} \frac{1}{\pi^2} \int_0^{k_F^l} \sqrt{k^2 + m_l^2} k^2 dk, \quad (21)$$

$$P_{\text{QP}} = \sum_{i=u,d,e,\mu} n_i \mu_i - \varepsilon_{\text{QP}}. \quad (22)$$

4 Hadron-quark phase transition

In this section, we study the hadron-quark phase transition which may occur in the core of massive neutron stars. It has been discussed extensively in the literature that a mixed phase of hadronic and quark matter could exist over a finite range of pressures and densities according to the Gibbs criteria for phase equilibrium. In the mixed phase, the local charge neutrality condition is replaced by a global one. This means that both hadronic and quark matter are allowed to be separately charged. The condition of global charge neutrality is expressed as

$$\chi n_c^{\text{QP}} + (1 - \chi) n_c^{\text{HP}} = 0, \quad (23)$$

where χ is the volume fraction occupied by quark matter in the mixed phase, which monotonically increases from $\chi = 0$ in the pure hadronic phase to $\chi = 1$ in the pure quark phase. n_c^{HP} and n_c^{QP} denote the charge densities of hadronic phase and quark phase, respectively. Without the constraint of local charge neutrality, we impose that the two phases are in weak equilibrium and described by two independent chemical potentials (μ_n, μ_e). The Gibbs condition for phase equilibrium at zero temperature is then given by

$$P_{\text{HP}}(\mu_n, \mu_e) = P_{\text{QP}}(\mu_n, \mu_e). \quad (24)$$

Using Eq. (24) we can calculate the equilibrium chemical potentials of the mixed phase where $P_{\text{HP}} = P_{\text{QP}} = P_{\text{MP}}$ holds. The energy density and the baryon density in the mixed phase are given by

$$\varepsilon_{\text{MP}} = \chi \varepsilon_{\text{QP}} + (1 - \chi) \varepsilon_{\text{HP}}, \quad (25)$$

and

$$n_{\text{B}}^{\text{MP}} = \chi n_{\text{B}}^{\text{QP}} + (1 - \chi) n_{\text{B}}^{\text{HP}}. \quad (26)$$

We show in Fig. 1 the possible phase structure of neutron star matter by using the RMF model with four different parameter sets for hadronic phase and a two-flavor version of the NJL model for quark phase. In particular, we are interested in the influence of the hadronic EOS on the phase transition. The shaded regions correspond to the mixed phase. It is shown that a pure hadronic phase is favored at low density. The mixed phase appears at the critical density $n_{\text{B}}^{(1)}$ where the pressure of the pure hadronic phase becomes to be lower than the pressure of the mixed phase. The fraction of quark matter χ increases with

increasing density in the mixed phase, and it turns to be a pure quark phase at the critical density $n_{\text{B}}^{(2)}$ where the pressure of the pure quark phase is above the pressure of the mixed phase. The critical densities $n_{\text{B}}^{(1)}$ and $n_{\text{B}}^{(2)}$ are model-dependent. We obtain $n_{\text{B}}^{(1)} = 0.37, 0.48, 0.50, 0.62 \text{ fm}^{-3}$ and $n_{\text{B}}^{(2)} = 0.83, 1.23, 1.06, 1.59 \text{ fm}^{-3}$ for the four RMF parameter sets NL3, TM1, GM1, and GPS used in the calculation. In order to estimate the influence of hadronic EOS on the deconfinement phase transition, we plot in Fig. 2 the four hadronic EOS and the NJL EOS with local charge neutrality as a function of the neutron chemical potential μ_n . The crossing of the hadronic EOS

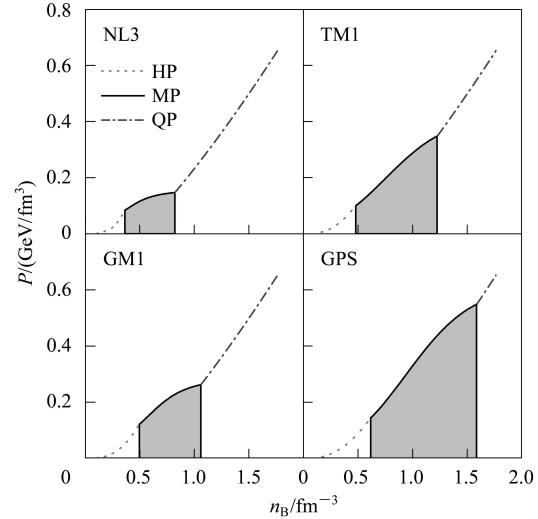


Fig. 1. The pressure P as a function of the baryon density n_{B} . The RMF model with four parameter sets NL3, TM1, GM1, and GPS is adopted for the hadronic phase (HP), while a two-flavor version of the NJL model is used for the quark phase (QP). The shaded regions correspond to the mixed phase (MP).

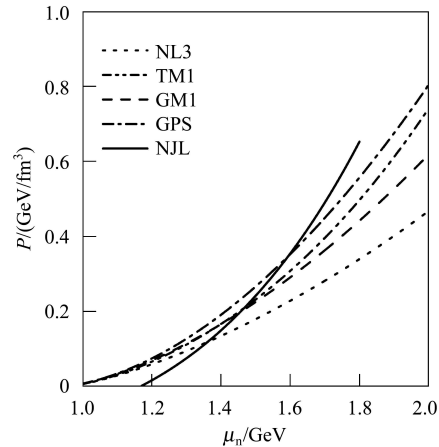


Fig. 2. The pressure P as a function of the neutron chemical potential μ_n for the charge neutral hadronic matter and quark matter. The parameter sets NL3, TM1, GM1, and GPS are adopted in the RMF model for the hadronic matter, and the NJL model is used for the quark matter.

and NJL EOS marks the transition point between the charge neutral hadronic matter and quark matter. It is seen that a harder hadronic EOS favors the phase transition at a lower μ_n . A more realistic treatment of the phase transition is to release the constraint of local charge neutrality, which leads to the existence of the mixed phase of charged hadronic and quark matter over a finite range of pressures and densities as shown in Fig. 1. In general, a harder hadronic EOS also favors an earlier appearance of the mixed phase.

In Fig. 3 we plot the full EOS in the form $P = P(\varepsilon)$, which consists of three parts: (a) the charge neutral hadronic matter phase at low density given by Eqs. (10) and (11), (b) the mixed phase of charged hadronic and quark matter described by Eqs. (23)—(26), (c) the charge neutral quark matter phase at high density given by Eqs. (21) and (22). The mixed phase part of the EOS is shaded gray, where the pressure varies continuously. It is shown that the onset and width of the mixed phase depend on the RMF parameter set used in the calculation. The NL3 parameter set leads to earlier appearance of the mixed phase and pure quark phase than the other three parameter sets, since the EOS with NL3 parameter set is harder than the other cases. The TM1 and GM1 parameter sets give almost the same threshold of the mixed phase, but different onset of the pure quark phase. This is because the hadronic EOS with GM1 parameter set gets harder than that with TM1 as density increases, and harder hadronic EOS favors earlier appearance of quark phase. The use of the four different parameter sets reflects the influence of the hadronic EOS on the hadron-quark phase transition, and it shows that the RMF parameter set plays an important role in this study.

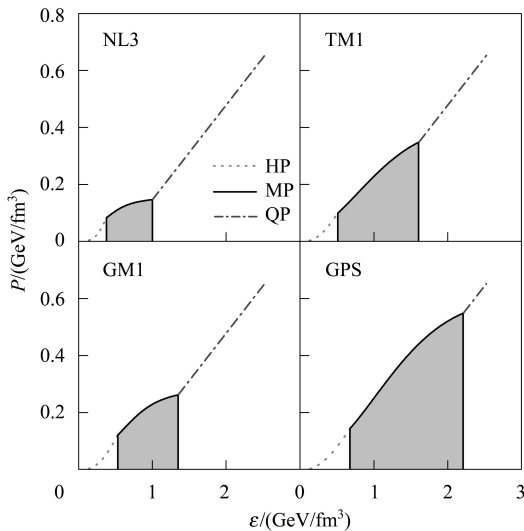


Fig. 3. The full EOS of neutron star matter in the form of pressure versus energy density. The shaded regions correspond to the mixed phase.

In Fig. 4 we show the particle fraction $Y_i = n_i/n_B$ as a function of the total baryon density n_B . Muons appear when the chemical potential of electrons exceeds the rest mass of muons. The fractions Y_p , Y_e , and Y_μ increase with increasing density before the mixed phase occurs. The quarks appear at the critical density $n_B^{(1)} = 0.37, 0.48, 0.50, 0.62 \text{ fm}^{-3}$ for the four parameter sets NL3, TM1, GM1, and GPS, then the fractions Y_u and Y_d increase rapidly with increasing density. At the critical density $n_B^{(2)} = 0.83, 1.23, 1.06, 1.59 \text{ fm}^{-3}$ for NL3, TM1, GM1, and GPS, the hadronic matter completely disappears where the pure quark phase occurs. Y_d is approximately twice of Y_u in the pure quark phase, and a small amount of electrons exist so as to maintain charge neutrality.

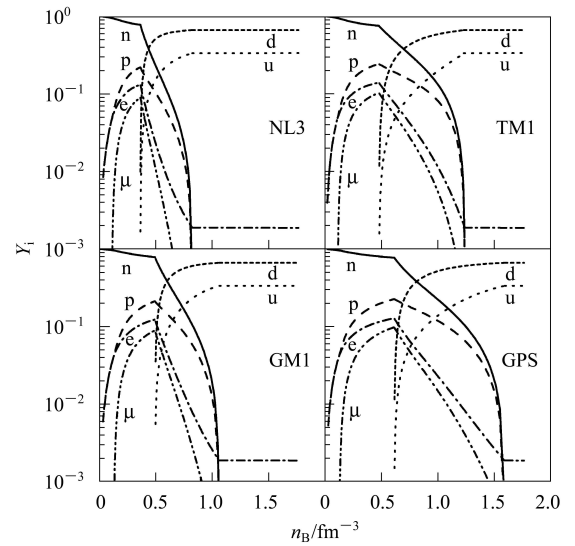


Fig. 4. The particle fraction $Y_i = n_i/n_B$ as a function of the total baryon density n_B .

5 Neutron star properties

In this section, we investigate the properties of neutron stars by solving the Tolman-Oppenheimer-Volkoff equation with the EOS over a wide density range. For the nonuniform matter at low density, which exists in the inner and outer crusts of neutron stars, we adopt a relativistic EOS based on the RMF theory with a local density approximation^[13, 14]. The nonuniform matter is modelled to be composed of a lattice of spherical nuclei immersed in an electron gas with or without free neutrons dripping out of nuclei. The low density EOS is matched to the EOS of uniform hadronic matter at the density where they have equal pressures. The pure hadronic phase ends at the critical density $n_B^{(1)}$, and the pure quark phase starts at the critical density $n_B^{(2)}$. The values of these critical densities depend on the RMF parameter set used in the calculation. The neutron star properties are

mainly determined by the EOS at high density. We calculate the neutron star profiles in order to examine whether or not quark matter can exist in the core of neutron stars.

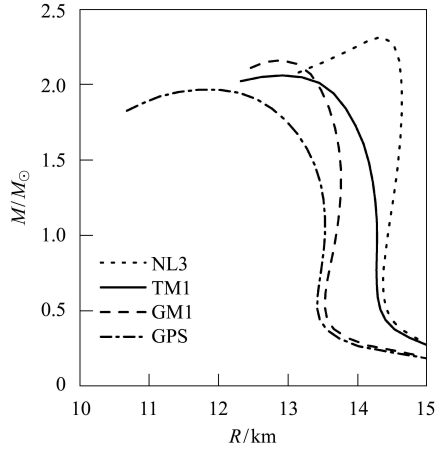


Fig. 5. The mass-radius relation for neutron stars.

In Fig. 5 we present the mass-radius relation using the EOS with the four different parameter sets of the RMF model. It is shown that the results depend on the parameter set significantly, and a harder hadronic EOS predicts a larger maximum mass of neutron stars. Since the pressure and density inside neutron stars decrease from the center to the surface, the most possible region where deconfined quark phase can exist is the center of the neutron star with maximum mass. We list in Table 3 the properties of neutron stars with maximum mass. It is found that the central baryon density n_c is between $n_B^{(1)}$ and $n_B^{(2)}$ for all parameter sets used in the calculation.

This means that the neutron star can possess a mixed phase core, but it is not dense enough to possess a pure quark core. In order to see the influence of the hadronic EOS on the neutron star properties, we show in Fig. 6 the neutron star profile with maximum mass for the four RMF parameter sets. The shaded regions correspond to the mixed phase cores of neutron stars. It is found the density distribution depends on the RMF parameter set. The thickness of the mixed phase core is about 5 km for all parameter sets used in the calculation.

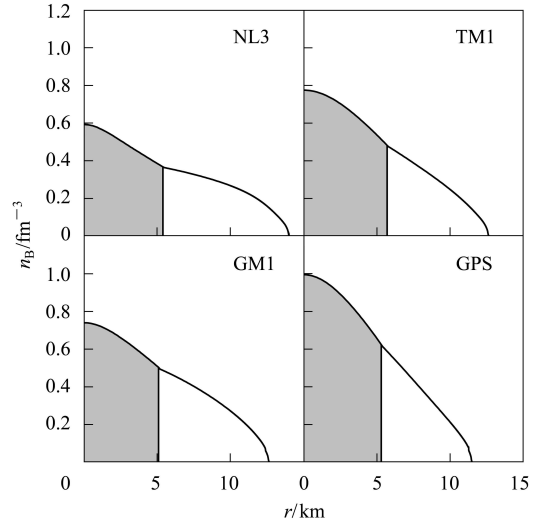


Fig. 6. The baryon number density n_B as a function of the radius r in neutron stars with the maximum mass listed in Table 3. The shaded regions correspond to the mixed phase cores of neutron stars.

Table 3. The properties of neutron stars with the maximum mass M_{\max} for the RMF parameter sets used in the calculation. The central energy density, pressure, and baryon number density are denoted by ε_c , P_c , and n_c , respectively. R and R_{MP} denote the radii of the star and its mixed phase core.

set	M_{\max}/M_{\odot}	$\varepsilon_c/(10^{15} \text{ g/cm}^3)$	$P_c/(10^{35} \text{ dyn/cm}^2)$	n_c/fm^{-3}	R/km	R_{MP}/km
NL3	2.3146	1.2168	2.0849	0.5923	14.330	5.405
TM1	2.0596	1.6315	3.3044	0.7749	12.920	5.704
GM1	2.1606	1.5512	3.3044	0.7400	12.905	5.105
GPS	1.9654	2.1793	5.2371	0.9953	11.730	5.305

6 Summary

We have studied the hadron-quark phase transition at high density, which may occur in the core of massive neutron stars. In the present work, we have adopted the RMF theory to describe the hadronic matter phase, while a two-flavor version of the NJL model has been used for the quark matter phase. In order to examine the influence of the hadronic EOS on the hadron-quark phase transition and neutron star properties, we have employed four RMF parameter sets, NL3, TM1, GM1, and GPS, which were fitted

to nuclear matter properties or ground-state properties of finite nuclei. The hadron-quark phase transition can proceed through a mixed phase of hadronic and quark matter over a finite range of pressures and densities according to the Gibbs criteria for phase equilibrium. We have found that the mixed phase starts at $n_B^{(1)} = 0.37, 0.48, 0.50, 0.62 \text{ fm}^{-3}$ and ends at $n_B^{(2)} = 0.83, 1.23, 1.06, 1.59 \text{ fm}^{-3}$ for the four parameter sets, NL3, TM1, GM1, and GPS, respectively. The use of the four different parameter sets reflects the influence of the hadronic EOS on the hadron-quark phase transition. In general, a harder hadronic EOS favors an earlier appearance of deconfined quark

matter.

We have calculated the properties of neutron stars using the EOS over a wide density range. The star properties such as their masses and radii are mainly determined by the EOS at high density. We found the maximum mass of neutron stars falls in the range $1.97 \sim 2.31 M_{\odot}$ for the four RMF parameter sets used in the present calculation, and their central baryon density is between $n_{\text{B}}^{(1)}$ and $n_{\text{B}}^{(2)}$. Therefore, the mixed phase can exist in the core of massive neutron stars, but no pure quark phase in the present approxima-

tion. We found the maximum mass and the density distribution inside neutron stars depend on the RMF parameter set adopted in the calculation. In the present work, the hadronic matter is restricted to nucleonic degrees of freedom in order to focus on the influence of the RMF parameter set on the hadron-quark phase transition. It would be interesting and important to incorporate other degrees of freedom such as hyperons and kaon condensation in the study of the hadron-quark phase transition in neutron stars.

References

- 1 Weber F. Prog. Part. Nucl. Phys., 2005, **54**: 193—288
- 2 Glendenning N K. Phys. Rev. D, 1992, **46**: 1274—1287
- 3 Heiselberg H, Hjorth-Jensen M. Phys. Rep., 2000, **328**: 237—327
- 4 Schaffner J, Mishustin I N. Phys. Rev. C, 1996, **53**: 1416—1429
- 5 Schertler K, Leupold S, Schaffner-Bielich J. Phys. Rev. C, 1999, **60**: 025801
- 6 Steiner A W, Prakash M, Lattimer J M. Phys. Lett. B, 2000, **486**: 239—248
- 7 Burgio G F, Baldo M, Sahu P K et al. Phys. Rev. C, 2002, **66**: 025802
- 8 Serot B D, Walecka J D. Adv. Nucl. Phys., 1986, **16**: 1—327
- 9 Gambhir Y K, Ring P, Thimet A. Ann. Phys., 1990, **198**: 132—179
- 10 Hirata D, Sumiyoshi K, Carlson B V et al. Nucl. Phys. A, 1996, **609**: 131—146
- 11 REN Z Z, TAI F, CHEN D H. Phys. Rev. C, 2002, **66**: 064306
- 12 SHEN H, YANG F, Toki H. Prog. Theor. Phys., 2006, **115**: 325—335
- 13 SHEN H, Toki H, Oyamatsu K et al. Nucl. Phys. A, 1998, **637**: 435—450
- 14 SHEN H. Phys. Rev. C, 2002, **65**: 035802
- 15 Lalazissis G A, König J, Ring P. Phys. Rev. C, 1997, **55**: 540—543
- 16 Sugahara Y, Toki H. Nucl. Phys. A, 1994, **579**: 557—572
- 17 Glendenning N K, Moszkowski S A. Phys. Rev. Lett., 1991, **67**: 2414—2417
- 18 Ghosh S K, Phatak S C, Sahu P K. Z. Phys. A, 1995, **352**: 457—466
- 19 Buballa M. Phys. Rep., 2005, **407**: 205—376
- 20 Vogl U, Weise W. Prog. Part. Nucl. Phys., 1991, **27**: 195—272
- 21 Hatsuda T, Kunihiro T. Phys. Rep., 1994, **247**: 221—367
- 22 Shovkovy I, Hanauske M, HUANG M. Phys. Rev. D, 2003, **67**: 103004